

PREPARATION AND PHOTOCATALYTIC ACTIVITY OF FLUORINE DOPED WO₃ UNDER UV AND VISIBLE LIGHT

G. H. JIN*, S.Q LIU

School of Chemistry and Chemical Engineering, Central South University, Changsha 410083 China

Fluorine doped WO₃ powders were synthesized by solid-state sintering method. The prepared F-doped WO₃ particles were characterized by scanning electron microscope, X-ray diffractometer, X-ray photoelectron spectroscopy, and UV-vis diffuse reflectance spectra and so on. Experimental results indicated that F-doping did not change the phase of WO₃ significantly. Therefore, it wouldn't generate crystallographic shear planes which could increase the resistivity of catalyst. Doping of F could increase the amounts of adsorbed oxygen and convert W⁶⁺ to W⁵⁺ by charge compensation, which could increase the oxygen vacancies. And the oxygen vacancies could enhance the extrinsic absorption and electron mobility, thus, although F-doping did not cause significant red-shift in the basic absorption range of WO₃, the actual photocatalytic activity under visible light and ultraviolet (UV) irradiation is increased. The photocatalytic activity was evaluated by water splitting under artificial solar light. The F-doped WO₃ powder calcined at 500 °C demonstrated the highest photocatalytic activity for water splitting under both UV and visible light (VIS) irradiation. And the highest average oxygen evolution rate under UV (102.1 μmol·L⁻¹·g⁻¹·h⁻¹) is 1.27 times the value of that of undoped WO₃ (80.2 μmol·L⁻¹·g⁻¹·h⁻¹).

(Received August 29, 2016; Accepted November 1, 2016)

Keywords: Fluorine-doped; Photocatalysis; Tungsten oxide; Water splitting

1. Introduction

After Honda-Fujishima Effect was discovered in 1972 [1], the possibility of splitting water using semiconductor photocatalysts was confirmed. Then more and more attention had been drawn in this research field. WO₃ was initially used as a kind of material for photodecomposition of water by Hodes [2]. Compared with TiO₂, its smaller band gap (2.5~2.8 eV) guaranteed that WO₃ could absorb more solar energy thus larger photocurrent could be generated. Moreover, WO₃ has stability against photocorrosion [3] and satisfactory photoelectron transport properties [4]. Besides, it is an effective photocatalyst for the evolution of oxygen.

The use of WO₃ as a stable photocatalyst for splitting of water has been reported by many investigators. Sayama[5] indicated that water could be completely decomposed into oxygen by WO₃ in the redox system of Fe³⁺/Fe²⁺ under visible light radiation, and Fe³⁺ was turned into Fe²⁺ gradually which could be then converted into Fe³⁺ again under UV radiation, and in this process, hydrogen could be produced thus complete decomposition of water could be realized by this circulation. Bamwenda [6, 7] found that with the aid of WO₃ and Ce⁴⁺/Ce³⁺ in the similar system, the production of hydrogen and oxygen could also be realized separately.

As a matter of fact, satisfied photocatalysts for splitting water are stringent. The material must be chemically inert and should have a band gap that can make use of an optimum of the solar spectrum (~ 1.6 eV) effectively. In addition, the semiconductor must be conducting and when placed in an electrolyte it should have sufficient band bending to separate the photogenerated

*Corresponding author: guanhuajin@foxmail.com

electron-hole pairs. The degree of band bending and the position of the bands can be modified to some degree by varying electrolyte and by the application of an external bias. It is known that the conductivity and band gap of such materials can be altered by chemical substitution or doping procedures [8-10]. Doping of some metal ions could promote photocatalytic efficiency, but metal-doped semiconducting oxides are generally thermo-labile, and could also introduce recombination between photogenerated electrons and holes [11]. So, doping of nonmetal elements attracts much attention. Asahi [12] demonstrated firstly the possibility of modification by doping nonmetal elements into TiO_2 through theoretical calculation, and three conditions that should be satisfied were proposed. Some researchers [9, 13, 14] reported the influence of doping N on WO_3 and found that the doping could significantly narrow the band gap to lower than 2.0 eV, which could greatly improve the photo absorption performance of WO_3 but the actual photocurrent became smaller than that of undoped WO_3 , they claimed that the poor photocurrent for N-doped sample was attributed to a degradation of the electron transport properties as a result of a highly defective lattice. Thus, to enhance conductivity of photocatalyst is important. Many experimental results showed that doping fluorine can decrease electrical resistance of semiconductors efficiently.

Though the F-doping WO_3 for photodecomposition of water has not been reported, many researchers have reported the possibility of the F-doping in TiO_2 modification [15-17]. Since the photo-reactivity of F-doped TiO_2 could be enhanced, similar considerations could be applied to WO_3 . It is expected that effective modification of WO_3 could be realized by fluorine doping.

In this study, a series of F-doped WO_3 samples with different amount of F was prepared by solid state reaction at low-heating temperature ($\sim 500^\circ\text{C}$). Samples were characterized by scanning electron microscope (SEM), X-ray diffractometer (XRD), X-ray photoelectron spectroscopy (XPS), and UV-vis diffuse reflectance spectra (DRS) techniques. Comparison with WO_3 , we focused on the influence of doping, calcined temperature and doping concentration on the properties of F-doped WO_3 powders and their photocatalytic activity under both ultraviolet and visible light irradiation. Experimental results showed that, with F-doped WO_3 as photocatalysts, in $\text{Fe}^{2+}/\text{Fe}^{3+}$ suspension, the highest oxygen production rate was $102.1 \mu\text{mol}\cdot\text{L}^{-1}\cdot\text{g}^{-1}\cdot\text{h}^{-1}$ ($\mu\text{mol O}_2$ per liter of suspension per gram of catalyst per hour) under ultraviolet irradiation, which was much higher than that of WO_3 , and the doping of F inhibited the photocatalytic activity under visible light to some extent.

2. Experimental

2.1. Preparation Process of WO_3 and F-doped WO_3 powders

Photocatalyst doped with F was prepared by low temperature solid-state sintering method. WO_3 powder used in this experiment was made by calcining ammonium tungstate for 5 hours at 600°C . A certain amount of NH_4F and WO_3 (1.0g) was mixed in organic aqueous solution according to the formula $m(\text{F})/m(\text{WO}_3)\times 100\%(\text{wt}\%) = \varepsilon\%$. After grinding in an agate mortar for 30 min, the sample was dried at 80°C in a thermostatic air-blower-driven drying closet. Then the prepared precursor were calcined for 2 h at the temperature of 200, 300, 400, 500, 600°C . FW-200~FW-600 are short for the samples calcined at different temperatures when $\varepsilon = 2.0$, and FW-0.5, FW-1.0, FW-2.0, FW-3.0 mean the samples calcined at 500°C when ε was in a range of $0.5\% \sim 3.0\%$.

2.2. Characterization of WO_3 and F-doped WO_3 photocatalysts

The morphology and size of F-doped WO_3 and WO_3 particles were observed by scanning electron microscope (SEM, JSM-5600LV, JEOL.LTD, Japan). The crystalline structure of the samples was measured by X-ray diffractometer (XRD, D/Max2250, Rigaku Corporation, Japan) using graphite monochromatic copper radiation ($\text{Cu K}\alpha$, $\lambda = 0.154056 \text{ nm}$) at 40kV, 300 mA. And the bonding energies were identified by X-ray photoelectron spectroscopy (XPS) with $\text{Mg K}\alpha$ radiation (energy = 1253.6 eV, 16 mA \times 12 kV) (XSAM800, Kratos, Britain), and all the bonding

energies were calibrated to the C_{1s} peak at 284.7 eV of the surface of adventitious carbon. Fluorine concentrations of F-doped WO₃ samples were measured by fluorine ion-selective electrode method. The resistivities were measured by 4-point probes resistivity measurement system (RST-9, Probes Tech. China). The UV-vis diffuse reflectance spectra (DRS) (versus BaSO₄) were recorded on a Pgeneral U-1901 spectrophotometer (China).

2.3. Photocatalytic property for oxygen evolution in water splitting

Photocatalytic reaction was carried out in a self-made hollow jacketed quartz reactor with an interior illuminant (high-pressure mercury lamp, emission wavelength of 300-400 nm, 250 W; high-pressure short arc xenon lamp, dominant frequency: 500 nm, 250 W). Two lamps served as simulated light sources of ultraviolet (UV) and visible light (VIS) irradiation respectively. Distilled water was boiled for 20 min before reaction to remove the air in the system. It was filled in reactor together with catalyst (3.57 g·L⁻¹) after it cooled down to the room temperature, and pH was kept at 2.0 at the beginning while the concentration of electron acceptor Fe³⁺ was 16.0 mmol·L⁻¹. Magnetic stirrer was employed to maintain the suspension of catalyst, and the reaction system was controlled at room temperature by external circulating water. The gas volume was determined by measuring the volume of spilled water.

3. Results and discussion

3.1 The morphologies of the WO₃ and F-doped WO₃ powders

The SEM images of FW-500 and WO₃ are shown in Fig. 1. The grain size was estimated to be in the region of 200 nm, with no significant variation when fluorine is incorporated. The unlisted SEM images of other samples are similar. This indicates that the calcined temperature has less effect on the shape and size of the F-doped WO₃ particles. After sintering for one more time no agglomeration was observed, this might be caused by restraint of F ions on the agglomeration by electrostatic repulsion [16].

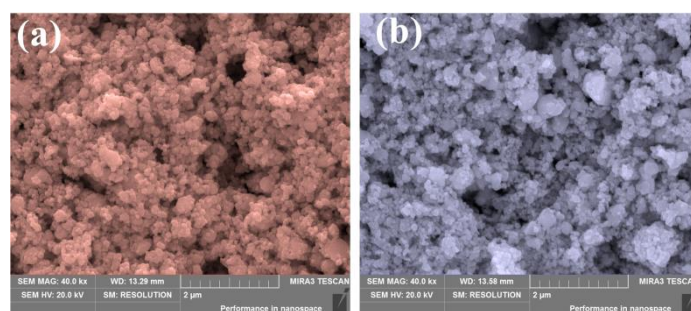


Fig. 1 SEM images of the (a) WO₃ and (b) F-doped WO₃ powders calcined at 500 °C

3.2 The crystal structures of the WO₃ and F-doped WO₃ powders

To investigate the structure, the WO₃ and F-doped WO₃ were evaluated by X-ray diffraction (as shown in Fig. 2). It can be noted that both WO₃ and F-doped WO₃ have significant diffraction peaks at 23.10°, 23.58° and 24.34° representing the characteristic of monoclinic tungsten oxide (PDF card # 72-0677). The three main peaks at ~23° are then attributed to the (002), (020), and (200) lattice planes of monoclinic WO₃. This could be easily understood that the ion radius of fluorine atom (0.133 nm) is virtually the same as the replaced oxygen atom (0.132 nm).

The grain sizes along [200] (D_{200}) of samples were calculated separately via the Scherrer formula and results were shown in Table 1. The grain sizes calculated from the Scherrer formula [18] based on the (200) peak was found to be 41.9 nm when calcinated at 200 °C, 43.2 nm at 300

°C 44.7 nm at 400 °C, 45.5 nm at 500 °C and 47.1 nm at 600 °C, that is, the grain size increased with increasing calcination temperature. Yang et al. [19] got the same conclusion in preparation of WO₃ samples by a sol-gel technique. In contrast, Sun et al. [20] found that grain size decreased with increased calcination temperature in their WO₃ samples prepared by spray pyrolysis method. We suppose these differences were due to the different synthetic method. In preparation of N doped WO₃ by Cole et al. [14], they found grain size decreased with the increase of the doping concentration, and Sun et al. [20] found for C doped WO₃, grain size increased with the increase of the doping concentration. In our research, when concentration of F increased, the grain size of different FW samples is similar (about 44.5 nm) without regular change. When it comes to the WO₃, the grain size is 34.8 nm; this might be attributed to that calcination was not favorable for the crystal refinement, as F-doped WO₃ samples were calcined twice [21].

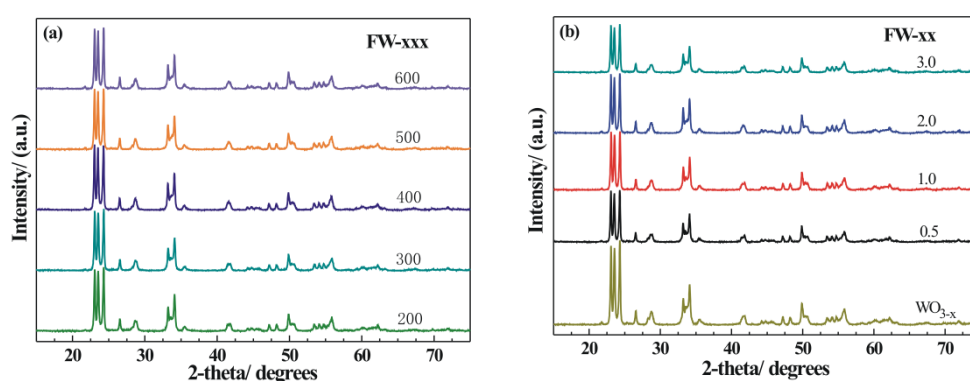


Fig. 2 XRD patterns of the (a) FW-200 ~FW-600, and (b) WO₃ and FW-0.5 ~FW-3.0

Although XRD spectra and grain size of F-doped WO₃ samples at different doping concentrations do not show apparent difference, in this study photocatalytic activity indeed exhibits variance. So some subtle differences should be observed. Marsen [22] pointed out that samples made under the same nominal conditions often exhibited significantly different photoelectrochemical response characteristics, which means some subtle changes would cause large differences, to make clear influence of these subtle, higher resolution diffraction methods are necessary.

Table 1. Material properties for WO₃ and F-doped WO₃ powders

Sample	D ₂₀₀ (nm)	F (at.%)	Resistivity (Ωcm)	AOER UV ^a	AOER VIS ^b
WO ₃	34.8	0.00	135.8	80.2	48.9
FW-0.5	45.7	0.04	124.5	96.1	55.5
FW-1.0	45.3	0.09	96.8	102.1	71.5
FW-2.0	45.5	0.21	38.2	87.3	60.3
FW-3.0	45.8	0.25	10.7	81.6	52.7
FW-200	41.9	-	-	73.0	22.7
FW-300	43.2	-	-	83.0	36.3
FW-400	44.7	-	-	84.4	43.5
FW-500	45.5	0.21	38.2	87.3	60.3
FW-600	47.1	-	-	80.1	15.1

^{a, b} Average oxygen evolution rates (μmol·L⁻¹·g⁻¹·h⁻¹) under UV and VIS irradiation.

3.3 The compositions of the WO₃ and F-doped WO₃ powders

The XPS survey spectra of WO₃ and F-doped WO₃ powders indicated that the peaks related mainly to W and O elements. A high-resolution XPS spectrum of the F 1s region of F-doped WO₃ sample was measured and is presented in Fig. 3(A). A peak at 687.5 eV can be attributed to the doped F-atoms in the WO₃, which is close to the value reported for substitutional F-atoms in TiO₂ [23]. This confirms that F-atoms are doped into the oxygen sites of the WO₃ crystal lattice

For both WO₃ and F-doped WO₃, on the O 1s region of XPS spectrum, an unsymmetrical O 1s peak was observed. This means that two chemical forms of O-atoms might exist in these powders. Therefore, using Gaussian distributions, the O 1s peak of samples was deconvoluted into two separated peaks. Fig. 3(B) gives the fitting result of O 1s region of WO₃ and FW-2.0. The O 1s region is composed of two contributions. The main contribution is the oxygen in the lattice (O²⁻) whose banding energy is 530.30 eV [24], and the minor contribution is assigned to adsorbed oxygen in the form of -OH on the surface whose banding energy is 531.10 eV [25]. As shown in Fig. 3(C), to reproduce the W 4f spectra, two doublet peaks and the Shirley background are combined. The highest-intensity doublet peak, labeled as a1 and a2, with binding energies of ~35.5 eV for (a1, W 4f_{7/2}) and ~37.45 eV (a2, W 4f_{5/2}) is associated with photoelectrons emitted from W atoms with +6 oxidation state (W⁶⁺). The other doublets in the spectra correspond to tungsten suboxides. The doublet found at ~0.9 eV lower binding energy (labeled as b1 and b2) is generated by photoelectrons emitted from W atoms with +5 oxidation state (W⁵⁺). All these binding energies (as shown in Table 2) were in agreement with the literature values for WO₃ [24, 26, 27]. According to the literature [28], the intensity ratio of the 4f_{5/2} to the 4f_{7/2} component is fixed to be 0.75 ($I[4f_{5/2}]/I(4f_{7/2}) = 0.75$) when fitting W 4f spectra.

Based on the XPS spectra, the contents of lattice oxygen (O (a)), adsorbed oxygen (O (b)), W⁶⁺ and W⁵⁺ on the surface of WO₃ and FW-2.0 were calculated and listed in Table 2. We could conclude that the doping caused an increase of W⁵⁺ and a decrease of W⁶⁺ on the surface of the catalysts.

Fluorine concentrations of F-doped WO₃ samples were measured by fluorine ion-selective electrode method as listed in Table 1. Fluorine content in all these samples was no higher than 0.25 at.%.

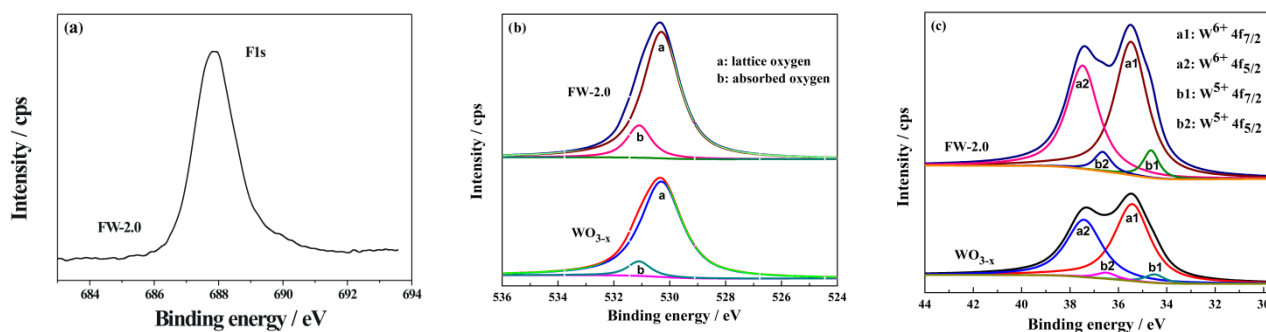


Fig. 3 XPS spectra for the (a)F 1s, (b) O 1s and (c) W 4f core levels of the WO₃ and FW-2.0

Table 2. Chemical composition of WO₃ and FW-2.0 calculated by XPS

Sample	O ²⁻		-OH		W ⁶⁺			W ⁵⁺		
	O (a)	%	O (b)	%	4f _{7/2}	4f _{5/2}	%	4f _{7/2}	4f _{5/2}	%
WO ₃	530.30	92.19	531.10	7.81	35.43	37.42	94.26	34.50	36.50	5.74
FW-2.0	530.30	85.52	531.10	14.48	35.48	37.48	91.02	34.65	36.65	8.98

3.4 The electronic properties of the WO₃ and F-doped WO₃ powders

Semiconductor resistivity is an expression of effective charge-separating and carrier mobility. As shown in Table 1, at increased precursor F concentration, the resistivity measured by 4-point probes measurements decreased from 135.8 Ωcm (WO₃) to 10.7 Ωcm (FW-3.0). Samples' photocatalytic activity could be directly influenced by resistivity. In literature [13, 14], doping of N lowered band gap of WO₃ and more solar energy should be absorbed, however, due to the increase of resistivity, the additional carriers generated upon illumination cannot be extracted, photocatalytic activity was greatly decreased. According to theoretical calculation by Asahi and Yamaki et al. [12, 29], in TiO₂, doping of F could not form intermediate energy levels below the conduction edge, which would improve the electron conductivity as doping of N. For WO₃, whether the intermediate energy levels could be formed by doping F needs further research.

Besides intrinsic properties and carrier concentration [13] of materials, grain size and oxygen vacancy are also factors that will influence resistivity. Grain size in the polycrystalline WO₃ plays a key role in establishing an effective charge-separating, the smaller the grains are, there will be the more grain boundaries, and these boundaries would impede free electrons transfer and thus the resistivity could be increased [14, 30].

Large amount of oxygen vacancies would generate crystallographic shear (CS) planes which could make resistivity increased [13, 14]. In our case, with reference to XRD analysis, this CS planes was not observed. Moreover, oxygen vacancies could serve as the traps of electrons and provide electrons, which are considered free and move through the material via polaronic transportation [14]. Considering that grain size of samples with different F concentration did not vary much, and more oxygen vacancies were found after doping, thus the decrease of resistivity is mainly caused by the increase of oxygen vacancies. Increase of adsorbed oxygen and substoichiometric WO₃ might generate more oxygen vacancies; this can be explained by F-doping, which converted W⁶⁺ to W⁵⁺ (XPS measurement) by charge compensation as supposed by Yu [15]. Meanwhile, carbonaceous residue from organic aqueous solution could act as a reducing agent to generate oxygen vacancies [31].

3.5 The absorption properties of the WO₃ and F-doped WO₃ powders

Diffuse reflectance spectroscopy (DRS) gives information about the absorption of the photocatalysts. In Fig. 4, the UV-vis reflectance of FW-0.5, FW-1.0, FW-2.0 and FW-3.0 are compared with WO₃. The absorption edges of all samples were at about 485 nm (2.56 eV). This value is close to that of pure WO₃, indicating that F-doping does not cause any significant red-shift in the fundamental absorption edge of WO₃.

This conclusion is partially similar to Asahi [12], Yamaki [29], Ho [23], Xu [32] and Li [33] et al. They believed that when doping with fluorine atoms in TiO₂, because of localized levels with high density below the VB of TiO₂, these levels consist of the F 2p state have no mixing with

VB or CB of TiO_2 . Accordingly, it is not expected to show high photocatalytic activity under visible light irradiation.

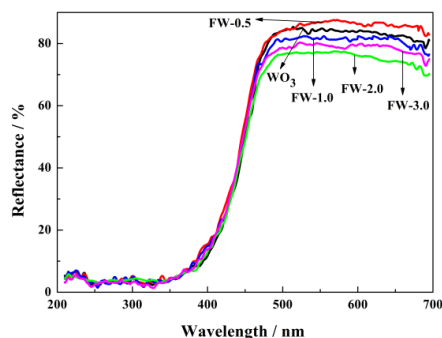


Fig.4 UV-vis diffuse reflectance spectra of WO_3 and FW with different amount of F

For WO_3 , certain amount of F doping could enhance the absorption of visible light, and the absorption value of FW-2.0 is the highest, when the doping amount was higher than 2.0%, absorption value decreased. And excessively high or low temperature does not benefit the increase of absorption rate of visible light (shown as Fig. 5).

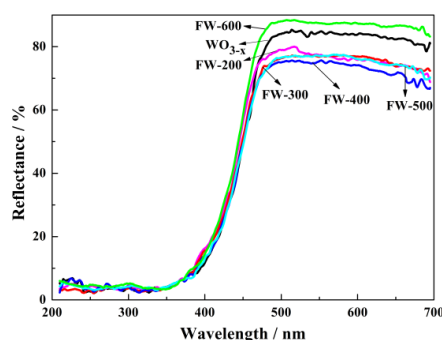


Fig. 5 UV-vis diffuse reflectance spectra of WO_3 and FW fabricated under different temperature

Actually, besides intrinsic absorption measured by DRS, surface state absorption and absorptions of different types of defects are also parts of actual absorption spectrum [34]. In previous research [17, 32, 33] in F-doped TiO_2 , extrinsic absorption through the existence of oxygen vacancies plays a decisive role in the improvement of catalytic activity.

3.6 Photocatalytic activities of the samples

Fig. 6 shows the average oxygen evolution rates of WO_3 and F-doped WO_3 with different doping amount for 12 hours under UV and VIS irradiation. The average oxygen evolution rates of F-doped WO_3 were higher than WO_3 under VIS, and this was in accordance with the results of absorption increase and resistivity decrease. Moreover, the photocatalytic activity of F-doped WO_3 samples also are higher than that of WO_3 under UV. Under UV, the average oxygen evolution amount of FW-1.0 reached the highest point of $102.1 \mu\text{mol}\cdot\text{L}^{-1}\cdot\text{g}^{-1}\cdot\text{h}^{-1}$ compared with $80.2 \mu\text{mol}\cdot\text{L}^{-1}\cdot\text{g}^{-1}\cdot\text{h}^{-1}$ of WO_3 , increased by 27%.

Generally, the observed activity of a photocatalyst is a combined effect of many factors including surface area, phase structure, oxygen vacancies and so on [33]. In our case, the precursor F concentration determined these factors because other conditions were identical. Therefore, it is easy to understand that the highest photocatalytic activity was obtained for a sample with a particular F concentration. Thus, although the absorption of UV irradiation did not change significantly, the factual photocatalytic activity was greatly improved by doping.

Moreover, extrinsic absorption increase and resistivity decrease are also the factors that improve photocatalytic activity, and it is possible that F doping could lead to enhancement of surface acidity and increase of active sites, both of which could also benefit photocatalytic performance [17, 33].

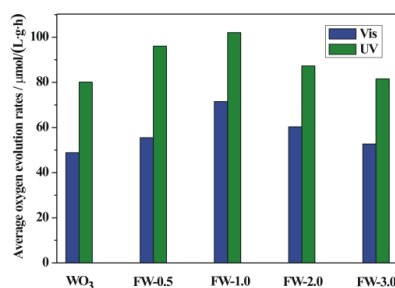


Fig. 6 Photocatalytic activity of WO₃ and FW with different amount of F for water splitting to oxygen under UV and VIS irradiation

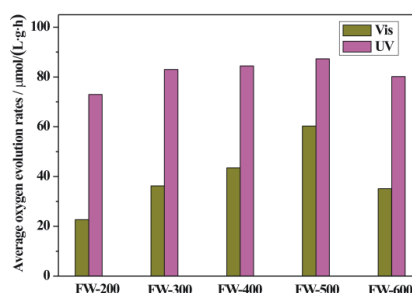


Fig.7 Photocatalytic activity of FW fabricated under different temperature for water splitting to oxygen under UV and VIS irradiation

Calcined temperature is also a combined factor when the F concentration is certain. As shown in Fig. 7, different calcined temperature has influence on the average oxygen evolution rates. When the temperature was excessively low or high, the photocatalytic activity would be negatively influenced and this might be explained as low temperature inhibited the doping of F into to the lattice of WO₃, while high temperature would promote the evaporation of nonmetal element F.

4. Conclusions

F-doped WO₃ was prepared by low temperature solid-state sintering method. The WO₃ and F-doped WO₃ are all monoclinic tungsten oxides, and the phase did not change significantly

when doped with F. Doping of F could increase the amount of adsorbed oxygen and W^{5+} on the surface and oxygen vacancies could be increased. Moreover, oxygen vacancies could reduce resistivity and increase extrinsic absorption. There was no significant red-shift in the fundamental absorption edge of WO_3 , but the absorption of visible light could be increased. Results of photocatalytic experiments show that, doping of F enhanced the photocatalytic activity under visible light and UV irradiation. With F-doped WO_3 as photocatalysts, in Fe^{2+}/Fe^{3+} suspension, the highest average oxygen evolution rate was $102.1 \mu\text{mol}\cdot\text{L}^{-1}\cdot\text{g}^{-1}\cdot\text{h}^{-1}$ under UV irradiation, which was much higher than that of WO_3 ($80.2 \mu\text{mol}\cdot\text{L}^{-1}\cdot\text{g}^{-1}\cdot\text{h}^{-1}$).

Acknowledgments

This study was supported by the Fundamental Research Funds for the Central Universities of Central South University (grants no. 2014zzts016).

References

- [1] A. Fujishima, K. Honda, *Nature* **238**, 37 (1972).
- [2] M.A. Butler, R.D. Nasby, R.K. Quinn, *Solid State Commun.* **19**, 1011 (1976).
- [3] D.E. Scaife, *Sol. Energy* **25**, 41 (1980).
- [4] J.M. Berak, M.J. Sienko, *J. Solid State Chem.* **2**, 109 (1970).
- [5] K. Sayama, R. Yoshida, H. Kusama, K. Okabe, Y. Abe, H. Arakawa, *Chem. Phys. Lett.*, **277**, 387 (1997).
- [6] G.R. Bamwenda, H. Arakawa, *Sol. Energy Mater. Sol. Cells* **70**, 1 (2001).
- [7] G.R. Bamwenda, T. Uesigi, Y. Abe, K. Sayama, H. Arakawa, *Appl. Catal. A: General*, **205**, 117 (2001).
- [8] X.C. Song, E. Yang, G. Liu, Y. Zhang, Z.S. Liu, H.F. Chen, Y. Wang, *J. Nanopart. Res.*, **12**, 2813 (2010).
- [9] Y. Liu, Y. Li, W. Li, S. Han, C. Liu, *Appl. Surf. Sci.*, **258**, 5038 (2012).
- [10] W. Li, F. Zhan, J. Li, C. Liu, Y. Yang, Y. Li, Q. Chen, *Electrochim. Acta* **160**, 57 (2015).
- [11] W. Choi, A. Termin, M.R. Hoffmann, *J. Phys. Chem.* **98**, 13669 (1994).
- [12] R. Asahi, T. Morikawa, T. Ohwaki, K. Aoki, Y. Taga, *Science* **293**, 269 (2001).
- [13] D. Paluselli, B. Marsen, E.L. Miller, R.E. Rocheleau, *Electrochem. Solid-State Lett.* **8**, G301 (2005).
- [14] B. Cole, B. Marsen, E.L. Miller, Y. Yan, B. To, K. Jones, M. Al-Jassim, *J. Phys. Chem. C* **112**, 5213 (2008).
- [15] J.C. Yu, J. Yu, W. Ho, Z. Jiang, L. Zhang, *Chem. Mater.* **14**, 3808 (2002).
- [16] G. Wu, A. Chen, *J. Photochem. Photobiol. A* **195**, 47 (2008).
- [17] D. Li, H. Haneda, N.K. Labhsetwar, S. Hishita, N. Ohashi, *Chem. Phys. Lett.* **401**, 579 (2005).
- [18] H. Song, H. Jiang, X. Liu, G. Meng, *J. Photochem. Photobiol. A* **181**, 421 (2006).
- [19] B. Yang, Y. Zhang, E. Drabarek, P.R.F. Barnes, V. Luca, *Chem. Mater.* **19**, 5664 (2007).
- [20] Y. Sun, C.J. Murphy, K.R. Reyes-Gil, E.A. Reyes-Garcia, J.M. Thornton, N.A. Morris, D. Raftery, *Int. J. Hydrogen Energy* **34**, 8476 (2009).
- [21] S.J. Hong, H. Jun, P.H. Borse, J.S. Lee, *Int. J. Hydrogen Energy* **34**, 3234 (2009).
- [22] B. Marsen, E.L. Miller, D. Paluselli, R.E. Rocheleau, *Int. J. Hydrogen Energy* **32**, 3110 (2007).
- [23] W. Ho, J.C. Yu, *Chem. Commun.* **2006**, 1115 (2006).
- [24] R. Huirache-Acuña, F. Paraguay-Delgado, M.A. Albiter, J. Lara-Romero, R. Martínez-Sánchez, *Mater. Character.* **60**, 932 (2009).
- [25] K. Shankar, G.K. Mor, H.E. Prakasam, S. Yoriya, M. Paulose, O.K. Varghese,

- C.A. Grimes, *Nanotechnology*, **18**, 065707 (2007).
- [26] A. Mozalev, V. Khatko, C. Bittencourt, A.W. Hassel, G. Gorokh, E. Llobet, X. Correig, *Chem. Mater.* **20**, 6482 (2008).
- [27] I.M. Szilagy, J. Madarasz, G. Pokol, P. Kiraly, G. Tarkanyi, S. Saukko, J. Mizsei, A.L. Toth, A. Szabo, K. Varga-Josepovits, *Chem. Mater.*, **20**, 4116 (2008).
- [28] L. Su, Q. Dai, Z. Lu, *Spectrochim. Acta, Part A*, **55**, 2179 (1999).
- [29] T. Yamaki, T. Umebayashi, T. Sumita, S. Yamamoto, M. Maekawa, A. Kawasuso, H. Itoh, *Nucl. Instrum. Methods Phys. Res. B*, **206**, 254 (2003).
- [30] E.L. Miller, B. Marsen, B. Cole, M. Lum, *Electrochem. Solid-State Lett.*, **9**, G248 (2006).
- [31] A. Hattori, K. Shimoda, H. Tada, S. Itos, *Langmuir*, **15**, 5422 (1999).
- [32] J. Xu, Y. Ao, D. Fu, C. Yuan, *Appl. Surf. Sci.* **254**, 3033 (2008).
- [33] D. Li, H. Haneda, S. Hishita, N. Ohashi, N.K. Labhsetwar, *J. Fluorine Chem.* **126**, 69 (2005).
- [34] A.V. Emeline, V.K. Ryabchuk, N. Serpone, *J. Phys. Chem. B* **103**, 1316 (1999).